

B14 ameliorates bone cancer pain through downregulating spinal interleukin-1 β via suppressing neuron JAK2/STAT3 pathway

Molecular Pain
Volume 15: 1–14
© The Author(s) 2019
Article reuse guidelines:
sagepub.com/journals-permissions
DOI: 10.1177/1744806919886498
journals.sagepub.com/home/mpx


Miao Xu^{1,2}, Huadong Ni², Longsheng Xu², Hui Shen²,
Housheng Deng², Yungong Wang³, and Ming Yao² 

Abstract

Curcumin has several pharmacological properties such as anti-inflammatory, antioxidant, and neuroprotective activities. B14 is a curcumin analogue and is considered to be a more potent compound with preserved pharmacodynamic activities. Based on the previous research studies, janus-activated kinase 2 (JAK2)/signal transducer and activator of transcription 3 (STAT3) signaling pathway plays a remarkable role in inflammation, chronic pain, and even contributes to the pathogenesis of neuropathic pain. Pro-inflammatory cytokines interleukin-1 β is a downstream factor of JAK2/STAT3 signal transition pathway, which participates in neuron injury and inflammation. We hypothesized that this signal transition pathway played an indispensable role in bone cancer pain. We herein established a bone cancer pain model to monitor the variation of JAK2/STAT3 signal transduction pathway and measured the effect of B14. The results in bone cancer pain model showed that (i) the levels of interleukin-1 β were elevated, and the ratios of p-JAK2/JAK2 and p-STAT3/STAT3 were increased; (ii) double immunostaining showed that p-JAK2, p-STAT3, and interleukin-1 β were colocalized primarily with neurons, rather than with astrocytes or microglial cells; (iii) B14 injection (intraperitoneally) markedly eased bone cancer pain; (iv) Western blotting showed that B14 injection lowered p-JAK2, p-STAT3, and interleukin-1 β levels, meanwhile the ratios of p-JAK2/JAK2 and p-STAT3/STAT3 was reduced; (v) immunofluorescence results also confirmed decreased levels of p-JAK2, p-STAT3, and interleukin-1 β in B14 treatment group. These findings suggested that B14 injection attenuated bone cancer pain in rats. This intervention inhibited JAK2/STAT3 cascade activation, downregulating interleukin-1 β expression in spinal dorsal horn.

Keywords

Curcumin derivative, bone cancer pain, JAK2/STAT3 signaling pathway, interleukin-1 β , neuron

Date Received: 27 May 2019; Revised 29 September 2019; accepted: 30 September 2019

Introduction

Bone metastasis generally occurs in the late stage of several cancer types, causing intolerant pain. Bone cancer pain (BCP) severely impacts the quality of life of the patients.¹ Currently, the World Health Organization analgesic ladder mainly includes opioids and nonsteroidal anti-inflammatory drugs and is considered as the primary treatment clinically.² Although other adjuvant therapies, such as surgery, radiotherapy, chemotherapy, nerve block technique, adoptive tumor immunotherapy, and antiepileptics are also used for BCP management, their effectiveness still remain a debatable topic.^{2,3}

¹The Second Affiliate Hospital and Yuying Children's Hospital, Wenzhou Medical University, Wenzhou, China

²Department of Anesthesiology and Pain Research Center, Jiaying University Affiliated Hospital, The First Hospital of Jiaying, Jiaying, China

³The Affiliated Zhuzhou Hospital Xiangya Medical College, Changsha, China

Corresponding Author:

Ming Yao, Department of Anesthesiology and Pain Research Center, Jiaying University Affiliated Hospital, The First Hospital of Jiaying, Jiaying 314001, China.

Email: jxyaoming666@163.com



So, more effective and rational treatment strategies for BCP are urgently needed.

Curcumin has been reported to have various intriguing bioactivities, but little has been studied regarding its use in multiple fields (Figure 1(a)).^{4–6} Researchers have paid much attention on neuroprotection, which is regarded as one of the remarkable characters of curcumin. Few studies on Parkinson's disease have demonstrated that curcumin treatment decreases and inhibits the deposition of misfolded α -synuclein accumulation in the brain cells.^{4,7} In addition, curcumin had the capability to alleviate inflammation by inhibiting microglial activation, reverse the distorted neuronal cells along with deposition of extracellular senile plaques of β -amyloid peptide (A β), and reduce the A β burden in serum and brain tissues of mice with Alzheimer's disease.^{8,9} Moreover, the antioxidant effect of curcumin has been used in the treatment of Alzheimer's disease.^{10–12} Previous studies have also revealed that curcumin could ease neuropathic pain by regulating IL-10.¹³ Also due to anti-inflammatory and antioxidant properties of curcumin, it has also been studied in Crohn's disease and ulcerative colitis.¹⁴ Based on its curative effects and deficiencies, all kinds of novel preparations and analogues were tailored. For instance, hyaluronic acid/curcumin nanomicelles were developed for treating rheumatoid arthritis, which enormously inhibited due to its inflammatory effect, and showed better bioavailability.¹⁰ B14 is a curcumin analogue and is synthesized by coupling appropriate aldehyde with acetone in an alkaline medium (Figure 1(b)).¹⁵ It has been proven that B14 had splendid medicinal effects when compared with curcumin.^{15,16} We herein explored the possibility of curcumin analogue B14 in treating BCP.

The janus-activated kinase (JAK)/signal transducers and activators of transcription (STAT) pathway contain 4 JAK and 7 STAT proteins.^{17,18} Some researchers have concluded JAK/STAT signaling pathway as a vital regulatory mechanism in basic biological functioning and disease progression of central nervous system.¹⁹ Further studies have demonstrated that JAK2/STAT3 signaling pathway plays a major role in N-methyl-D-aspartic acid receptor-dependent pain transmission and neuropathic pain.^{20–22} Meanwhile, in spared nerve injury (SNI)-induced neuropathic pain model, researchers have revealed activation of neuronal JAK2/STAT3 signaling pathway by upregulating the expression of N-methyl-D-aspartate receptor subunit 1 (NR1) that contributed to neuropathic pain.²³ Other studies have confirmed that JAK2/STAT3 cascade could be activated by cytokine ILs, such as IL-6, and chemokine (C-X-C motif) ligand 12, which are associated with inflammation.^{24–26}

IL-1 β is one of the common neuroinflammatory substances that greatly increase in neuropathic pain.²⁷ The composition of pro-IL-1 β can be initiated by JAK2/

STAT3 signaling pathway through toll-like receptors.²⁸ In addition, inflammasome oligomerization and caspase-1 auto-activation lead to caspase-1-dependent cleavage of pro-IL-1 β producing biologically active, mature IL-1 β .²⁹ According to a previous study, IL-1 β has been confirmed to have the ability to act as a neurotoxic mediator.³⁰ For example, upregulation of IL-1 β in the area of medial forebrain bundle remarkably decreased the number of dopaminergic neurons in the striatum.³¹ Other studies have showed that IL-1 β mediated neuronal apoptosis via p-38 mitogen-activated protein kinase activity after spinal cord injury.³² Curcumin has been demonstrated to downregulate IL-1 β to achieve neuroprotection.³³

The mechanism of BCP involves vast intracellular signal transduction pathways and a mass of extracellular signal conducting molecules.^{34–36} In our previous research study, various inflammatory signaling pathways and numerous inflammatory cytokines, such as nuclear factor kappa B (NF- κ B) signaling pathway, chemokine CC motif receptor-2 (CCR2), monocyte chemoattractant protein-1 (MCP-1), as well as nuclear protein high-mobility group box-1 (HMGB1) contributed significantly in the treatment of BCP.^{37,38} In this study, we attempted to demonstrate the curative effects of B14 on mitigating BCP and to investigate whether it downregulates JAK2/STAT3 signaling pathway in astroglial cells, causing decreased IL-1 β expression and maturation rate in the spinal cord.

Material and methods

Animals

Nine-weeks-old adult female Sprague-Dawley (SD) rats, weighing 180–200 g supplied by the Experimental Animal Center of Zhejiang Province Academy of Medical Sciences (Hangzhou, China) were used for all experimental operations. The rats were raised for five days in groups of four per cage under controlled conditions (22°C–25°C, 7 a.m. to 7 p.m. 12-h light/dark cycle) with food and water ad libitum. All experiments were performed according to the Ethical Guidelines for Investigations of Experimental Pain in Conscious Animals³⁹ and were approved by the Animal Use and Care Committee for Research and Education of the Jiaxing University.

Experimental procedure

The basic experimental procedure contains five main steps:

1. Establishment of BCP model, measurement of pain threshold, and radiography. SD rats were randomly distributed into naive, BCP and sham (injection

inactivated Walker 256 cell) groups. The paw withdrawal threshold (PWT) of the operation side was recorded on day 1 before and on days 1, 3, 6, 9, 12, 15, and 18 after operation. Meanwhile, on day 1 before, and on days 12 and 24 after operation, the rats in BCP group underwent computed tomography (CT) examination (Figure 2(a)).

- Confirmation of whether p-JAK2, p-STAT3, JAK2, STAT3 and IL-1 β were increased in BCP. SD rats were randomly divided into five groups: naive, sham, and BCP (6, 12, and 18 days) groups. Rats in each group were anesthetized and harvested at a certain time point for Western blotting ($n = 4$). Other SD rats were randomly distributed into three groups: naive, sham, and BCP groups. All rats were anesthetized and harvested on day 12 after operation to undergo immunohistochemistry and hematoxylin-eosin staining. The sample from the surgical paw was used for hematoxylin-eosin staining. The spinal cord from the BCP group was fluorescently labeled (p-JAK2, p-STAT3, and IL-1 β) and comarked with Iba-1 (the microglial marker), glial fibrillary acidic protein (GFAP) (the astrocytic marker), or NeuN (the neuronal marker), (Figure 2(b)).
- Measurement of 24 h pain threshold after injecting single dose of B14. SD rats were randomly distributed into six groups: naive, sham, and BCP (0, 2.5, 5, and 10 mg/kg) groups. B14 injection was given on day 12 after operation (solvent 2 ml 5% dimethylsulfoxide (DMSO), intraperitoneally (i.p.) once). The PWT on the operation side was recorded 1 h before and at 1, 2, 3, 4, 5, 6, 7, 8, 9, 10, 11, 12, 13, 16, 20, and 24 h after injection (Figure 2(c)).
- Measurement of long-term pain threshold after injection of multiple doses of B14. SD rats were randomly distributed into six groups: naive, sham, and BCP (0, 2.5, 5, and 10 mg/kg) groups. B14 injection was administered on day 6 after operation (i.p. qd. [quaque die]) for 1 week. The PWT on the operation side on days 0, 3, 6, 9, 12, 15, and 18 after surgery was recorded (Figure 2(d)).
- Confirmation of whether p-JAK2, p-STAT3, JAK2, STAT3, and IL-1 β was decreased in BCP after treatment. SD rats were randomly distributed into six groups: naive, sham, and BCP (0, 2.5, 5, and 10 mg/kg) groups. B14 injection was administered on day 6 after operation (i.p. qd.) for seven days. Rats in each group were anesthetized and harvested after reaching the peak value after last injection for Western blotting ($n = 4$). Additional SD rats were randomly distributed into three groups: naive and BCP (0 and 10 mg/kg). All rats were anesthetized and harvested on day 12 after injection and those samples were fluorescently labeled (p-JAK2, p-STAT3 and IL-1 β) and comarked with Iba-1, GFAP, or NeuN (Figure 2(e)).

Cell line

Rat-derived breast cancer cell line, Walker 256, was used in this experiment to establish BCP model. This was passaged from the original cell line and was generously presented by the Nanjing University of Chinese Medicine. This was widely used in our previous research studies.^{38,40,41}

BCP model

The establishment of BCP was vividly described in our previous papers.^{40,41} Female SD rats (except the naive group) were anesthetized with pentobarbital sodium (60 mg/kg, i.p.). In order to provide a clear view of the proximal tibia, an aseptic incision was gently made on the left leg. After careful drilling of a tiny hole on the exposed proximal tibia, the size of the needle that best fitted the Feige microsyringe was used. Walker 256 breast cancer cells (10 μ l, 1×10^6 /ml) or heat-inactivated Walker 256 breast cancer cells (10 μ l, 1×10^6 /ml) (sham group) were slowly injected into the marrow cavity. After waiting for a moment to balance the pressure, the microsyringe was removed, and then the hole was sealed with bone wax immediately. Finally, an aseptic incision was sutured with fibrin glue.

Drugs

B14 was generously presented by Wenzhou Medical University Second Affiliated Hospital. It was dissolved in DMSO (Sigma-Aldrich), diluted in saline to several appropriate concentrations, and then the final concentration of 5% DMSO was prepared. According to different doses, female SD rats were randomly divided into six groups: naive, sham, BCP + vehicle group, BCP + B14 2.5 mg/kg, BCP + B14 5 mg/kg, and BCP + B14 10 mg/kg. In each group, drugs were administered once in a fixed time point of the day (i.p.), starting from day 6 till day 12, consecutively for seven days.

Behavioral test

The mechanical allodynia of SD rats was tested by measuring the operative PWT using von Frey filaments (IITC, USA) in a blinded manner.^{42,43} During the test, each rat was isolated in a resin-glass partition (25 \times 20 \times 20 cm), with 0.5 \times 0.5 cm iron grids on the bottom. After five days of adapting to the laboratory conditions, the baseline characteristics were measured one day before the surgery to narrow the error. Next, the rats were placed in the resin-glass partition for 30 min per day for three days in advance. In the formal test, after 30 min of acclimatization, a pressure was vertically exerted on the plantar surface of the operated hind leg for 2–3 s between the two stimulations, with a time gap

of 5 min. The data were recorded until the positive signs were shown up (rapidly pull back or bit or lick or shake the tested hind leg). All the data collected were according to the laws of Dixon's up-down method. The value of PWT was calculated as an average of three values obtained from each stimulation.

CT reconstruction

For CT three-dimensional bone reconstruction, SIEMENS SOMATOM Definition AS, a CT scanner, was used. SD rats were anesthetized with pentobarbital sodium (60 mg/kg, i.p.) before undergoing the scan. The acquisition parameters were as follows: helical scanning, 120 kVp, Care dose 4D technique, layer thickness of 1 mm, layer interval of 1 mm, kernel: U30u medium smooth, with CT imaging of SD rat's tibia at high resolution (field of view 100 mm). All the images were processed and analyzed via Siemens Syngo MultiModality Workplace (MMWP) postprocessing workstation.

Pathological process

To observe histological alterations of BCP, the rats were administered with pentobarbital sodium overdose (100 mg/kg, i.p.) on day 12 of BCP. Tissues, with puncture point on the tibial bone as the center (0.5 cm around), were accurately removed and decalcified in 10% ethylenediaminetetraacetic acid mixture for 24 h and then embedded with paraffin. According to our previous study, a series of 8- μ m thick sagittal sections were cut across the entire tissues. After safranin-O/fast-green hematoxylin and eosin staining, the sections were observed under 200 \times microscope (OLYMPUS).

Western blot

SD rats were deeply anesthetized with pentobarbital sodium (60 mg/kg, i.p.), and then the L4–L5 segments of ipsilateral spinal cord were harvested. Sample tissues were subjected to sodium dodecyl sulfate polyacrylamide gel electrophoresis. Western blotting was conducted by probing these tissues with primary antibodies such as anti-JAK2 antibody, anti-p-JAK2 antibody, anti-STAT3 antibody, anti-p-STAT3 antibody, anti-IL-1 β antibody, and normalized with glyceraldehyde 3-phosphate dehydrogenase.

Immunofluorescent histochemistry

P-JAK2, p-STAT3, IL-1 β and NeuN, Iba-1, or GFAP in SD rats' spinal cord underwent double immunofluorescence labeling and visualized under a confocal microscope (Leica TCS SP2; Wetzlar, Germany). SD rats were anesthetized with pentobarbital sodium (60 mg/kg, i.p.) and transcardially perfused with 150 ml of

5 mM phosphate-buffered saline (PBS) (pH 7.4), followed by 100 ml of 4% (w/v) paraformaldehyde PBS. After sample isolation, spinal lumbar enlargements (L3–L5) are fixed in 4% (w/v) buffered paraformaldehyde for 6 h and dehydrated for 48 h in gradient sucrose solutions (15%–30%) at 4°C. These spinal samples were embedded in (optimal cutting temperature) OCT compound (Sakura, America) at –20°C and then were cut into 25 μ m sections. All frozen sections were washed thrice, 10 min each with 0.01M PBS. After that, the sections were blocked in 0.01M PBS containing 8% (v/v) donkey serum and 0.5% (v/v) Triton X-100 for 1 h at 28°C. Again, after washing the sections thrice for 10 min each in 0.01M PBS, they were incubated overnight with the following primary antibodies: anti-p-JAK2 antibody (1/100, rabbit, Abcam), anti-p-STAT3 antibody (1/100, rabbit, Cell Signaling Technology (CST)), anti-IL-1 β antibody (1/100, rabbit, affinity), Iba-1 antibody (1/100, mouse, Gene Tex), NeuN antibody (1/100, mouse, Abcam), and GFAP antibody (1/100, mouse, CST), in PBS containing 5% (v/v) donkey serum, at 4°C.

After incubating with primary antibodies, the sections were washed thrice as usual and then incubated at 28°C with donkey secondary antibodies (Cy3- or fluorescein isothiocyanate-conjugated secondary antibodies (1:500, Abcam)) for 2 h by shielding from light. Finally, the sections were flattened onto the glass slides, coverslipped with water-based mounting medium containing 4',6-diamidino-2-phenylindole (DAPI) (Bioss, China) and observed under a confocal microscope (Leica TCS SP2; Wetzlar, Germany). Each group was provided with four samples, and each sample has five sections from different rostrocaudal planes between L4 and L5. All the images were analyzed by Image Pro Plus 6.0 (Image Pro Plus Kodak, USA).

Statistical analyses

All data were processed by using SPSS version 20.0 and were presented as mean \pm standard deviation. One- or two-way analysis of variance (ANOVA) was used to calculate the data and detect the differences between the groups. The F test was used to examine the equality of variances in t test and Levene's equality of error variances for ANOVA. $p < 0.05$ was considered to be statistically significant.

Results

BCP model

After measuring the baseline characteristics, surgery was performed under moderate anesthesia, and the Walker 256 breast cancer cells (10 μ l, 1×10^6 /ml) were injected

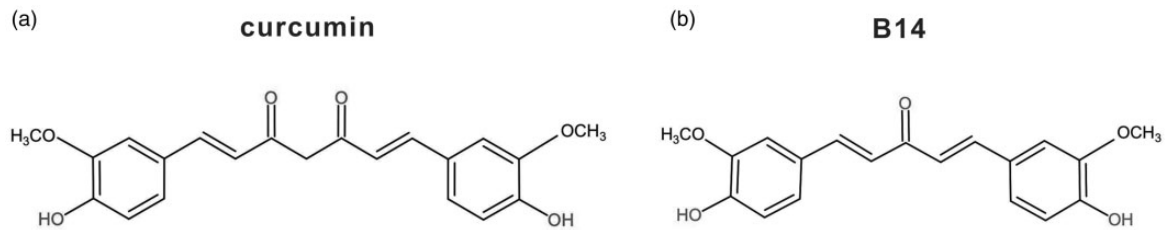


Figure 1. Chemical structure of curcumin (a) and B14 (b).

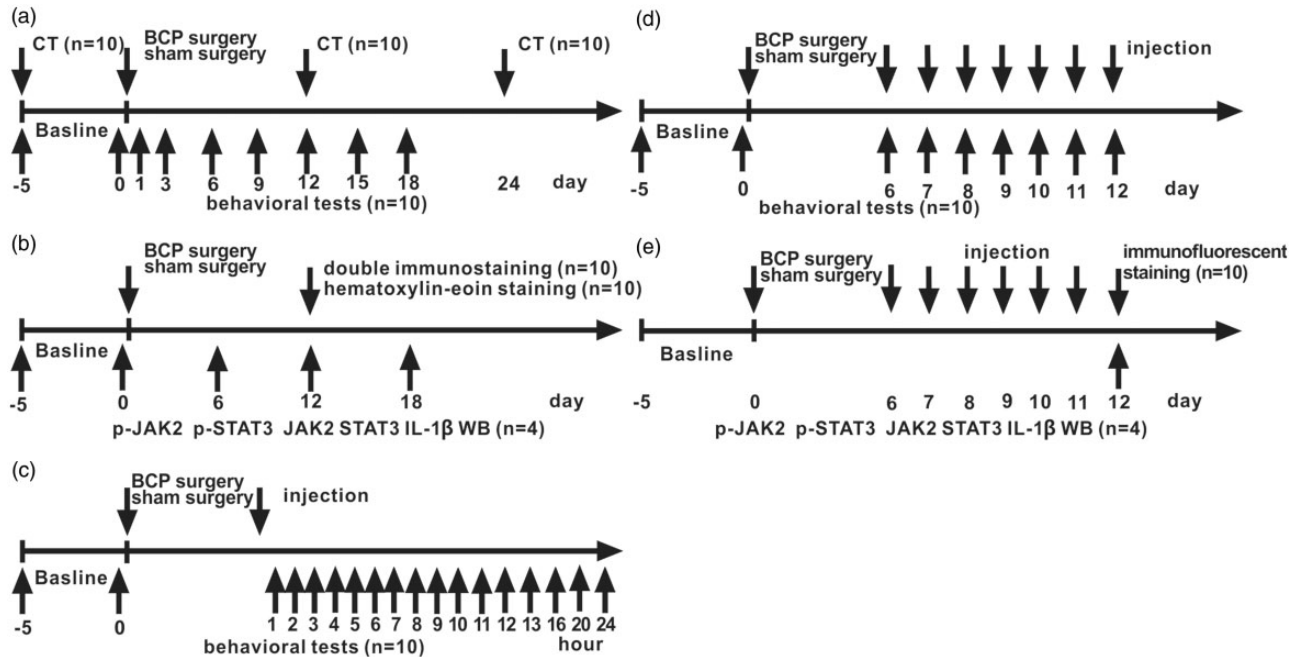


Figure 2. Experimental paradigms. CT: computed tomography; BCP: bone cancer pain; IL: interleukin; JAK2: janus-activated kinase 2; STAT3: signal transducer and activator of transcription 3; WB: Western blotting.

into the left tibia of SD rats as previously described (day 0). The rats in the sham group were injected with heat-inactivated Walker 256 breast cancer cells (10 μ l, 1×10^6 /ml). The naive group was exempted from surgery. Behavioral assessment was done on days 1, 3, 6, 9, 12, 15, and 18 after operation by PWT. In the BCP group, the quantitative value of PWT was decreased on day 6 after operation when compared to the naive group. The speed of the decrease was gentle on day 6 after operation ($F_{2,27} = 32.35$, $***p < 0.001$ vs. sham group; $n = 10$, two-way repeated measures ANOVA, Figure 3(b)). PWT showed no significant differences between the naive group and the sham group ($F_{2,27} = 32.35$, $p > 0.05$ vs. sham group; $n = 10$, two-way repeated measures ANOVA, Figure 3(b)). Based on the images, osteolysis and osteoproliferation were demonstrated to be anabolic with the development of BCP (Figure 3(a)). Under

optical microscope, the normal construction of bone trabecula showed severe destruction; and moreover, the marrow cavity was filled with cancer cells (Figure 3(c) and (d)).

Changes of JAK2, STAT3, p-JAK2, p-STAT3 and IL-1 β in BCP model

The JAK2/STAT3 signaling pathway showed massive activation in neuropathic pain. Furthermore, many researchers have found that activation of JAK2/STAT3 pathway showed positive associations with the mechanisms of neuropathic pain.⁴⁴ Here, Western blotting was performed to reveal the changes in the rules of JAK2, STAT3, p-JAK2, p-STAT3, and IL-1 β during the establishment of BCP, and the results regarding the ratios of p-JAK2, p-STAT3 with JAK2, and STAT3

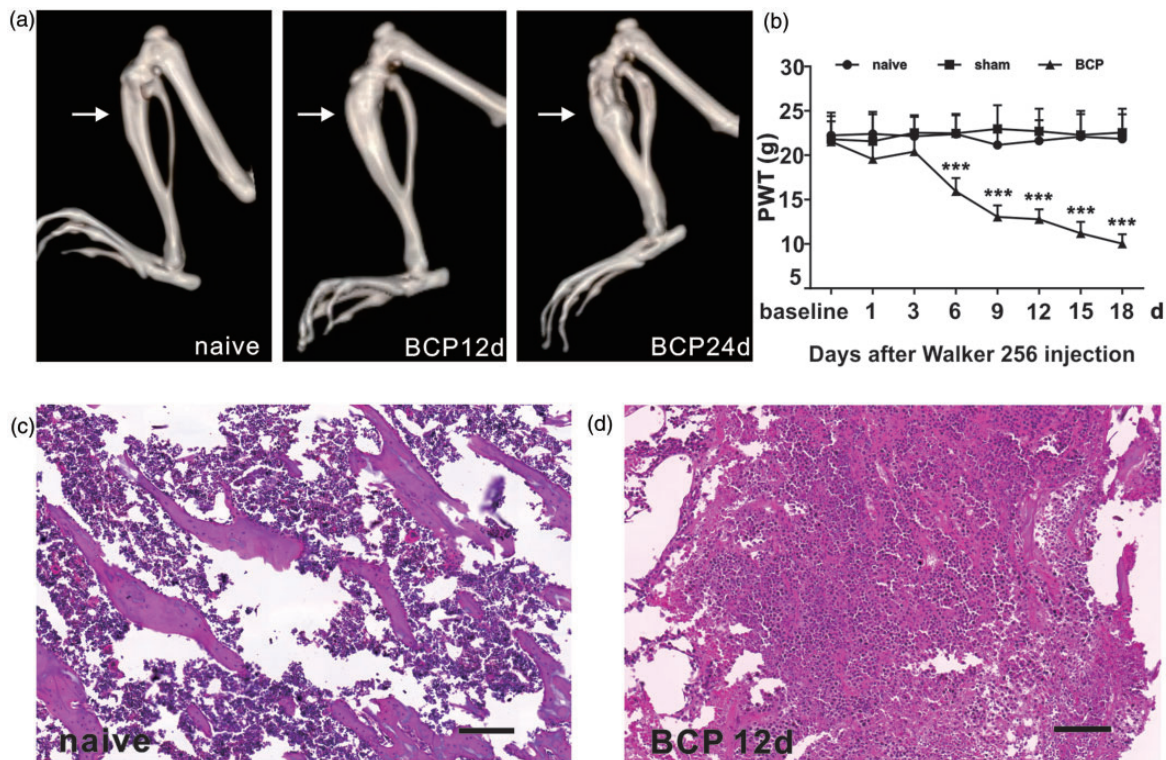


Figure 3. BCP-induced mechanical allodynia of hindpaw. (a) Three-dimensional rebuild CT image of the tibia bone after walker 256 cell injection showing cortical bone damage. Arrowhead points to the spot of tumor cells caused abnormal bone structure. (b) PWTs of ipsilateral hind paw remarkably decreased on BCP 6 days to 12 days, $n = 10$ per group, $***p < 0.001$ versus Naive group. Hematoxylin-eosin staining of bone destruction showing malignant tumor infiltration and bone trabecula destruction (d) compare to normal bone tissue (c), $n = 10$ per group. Scale bar: 100 μm . BCP: bone cancer pain; PWT: paw withdrawal threshold.

were gradually increased with BCP progression ($F_{4,15} = 30.14$, $***p < 0.001$ vs. sham group; $F_{4,15} = 40.97$, $***p < 0.001$ vs. sham group; $n = 4$, one-way ANOVA, Figure 4(a) to (d)). Downstream protein factor IL-1 β expression showed remarkable increase ($F_{4,15} = 37.55$, $***p < 0.001$ vs. sham group; $n = 4$, one-way ANOVA, Figure 4(e) and (f)).

Double immunofluorescent staining of P-JAK2, p-STAT3, and IL-1 β are primarily present in the neurons of spinal dorsal horn

On day 12 of BCP, all six groups: naive, sham, and BCP (0, 2.5, 5, 10 mg/kg) were harvested under deep anesthesia for Western blotting and immunofluorescence. Double immunostaining results showed that p-JAK2 in spinal dorsal horn was colocalized with astrocytes (Figure 5(a)), microglial cells (Figure 5(b)), and neurons (Figure 5(c)). Almost $64.5\% \pm 4.8\%$ showed colocalization with neurons, $16.3\% \pm 2.4\%$ p-JAK2 showed colocalization with astrocytes and around $19.3\% \pm 3.6\%$ with microglial cells (Figure 5(d)). Similarly, p-STAT3 showed colocalization with all three kinds of cells in

the spinal cord (Figure 5(e) to (g)) in which $84.0\% \pm 4.8\%$ was colocalized with neurons, $6.6\% \pm 2.6\%$ with astrocytes, and $9.4\% \pm 3.6\%$ with microglial cells (Figure 5(h)). The results of IL-1 β cellular colocalization in spinal cord dorsal horn revealed that IL-1 β was mostly colocalized with neurons (Figure 5(k)), and almost $77.4\% \pm 7.6\%$ (Figure 5(l)), with minor in astrocytes (Figure 5(i)) of $5.9\% \pm 3.4\%$ (Figure 5(l)) or microglial cells (Figure 5(j)) of $16.8\% \pm 5.7\%$ (Figure 5(l)).

i.p. injection of B14 improves mechanical allodynia in BCP rats

For testing the analgesic effects of *i.p.* injection of B14 in BCP rats more comprehensively, three doses (2.5, 5, and 10 mg/kg) of B14 were administered to rats in this experiment. All *i.p.* injections were administered on days 6, 7, 8, 9, 10, 11, and 12 after operation. The quantitative value of PWT of ipsilateral operational posterior limb was measured and recorded 1 h before and at 1, 2, 3, 4, 5, 6, 7, 8, 9, 10, 11, 12, 13, 16, 20, and 24 h after injection. Compared with control group, PWT was dramatically augmented at 6 h till 11 h in 5 mg/kg and 10 mg/kg B14-treated BCP

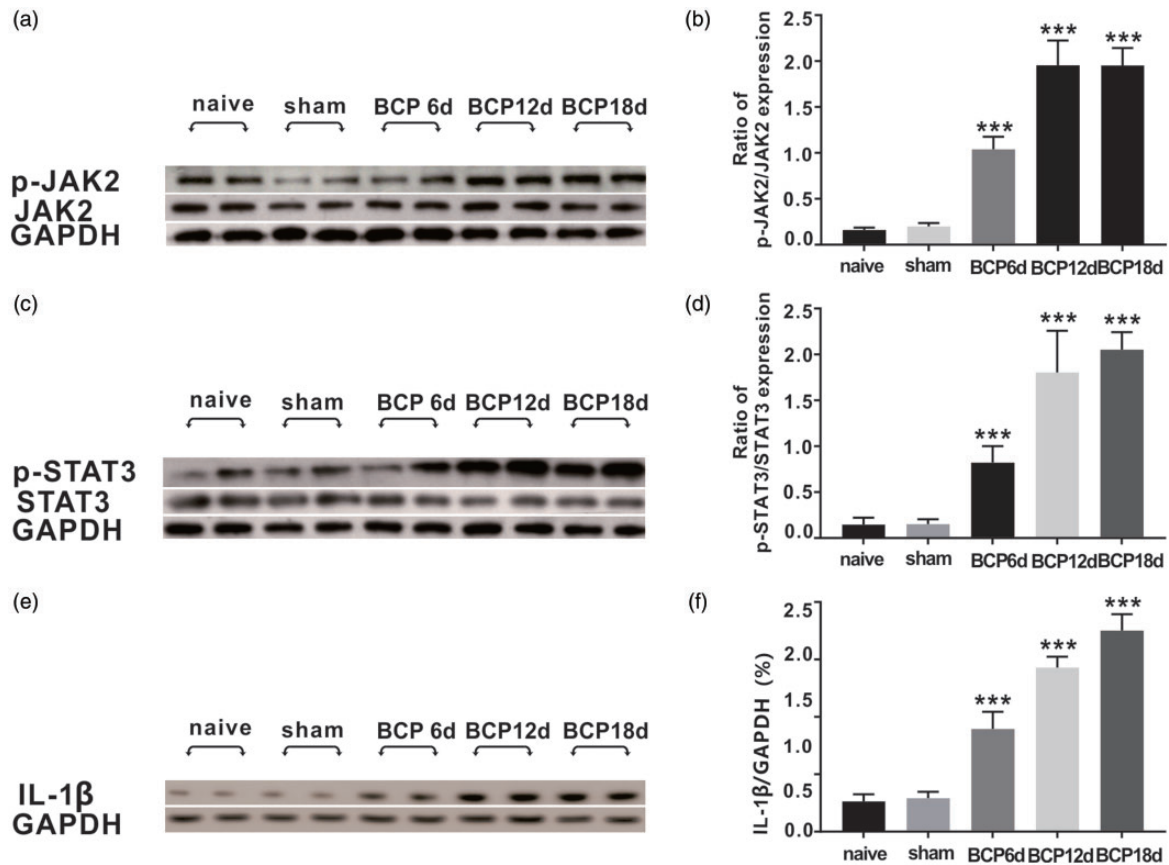


Figure 4. Variation tendency of p-JAK2, p-STAT3, JAK2, STAT3, and IL-1 β in BCP molding. (a to d) Western blot analysis showing the ratio of p-JAK2/JAK2 and p-STAT3/STAT3 expression were increasing dramatically with BCP molding, especially in BCP 12 days and BCP 18 days, $n = 4$ per group, $***p < 0.001$, $***p < 0.001$ versus sham group. (e and f) Spinal protein level of IL-1 β after walker 256 cell injection using Western blot analysis prominently elevated from BCP 6 days to BCP 18 days, $n = 4$ per group, $***p < 0.001$ versus sham group. BCP: bone cancer pain; GAPDH: glyceraldehyde 3-phosphate dehydrogenase; IL: interleukin; JAK2: janus-activated kinase 2; STAT3: signal transducer and activator of transcription 3.

groups and then showed a progressive decline ($F_{5,54} = 295.2$, $**p < 0.01$, $***p < 0.001$ vs. control; $n = 10$, two-way repeated measures ANOVA, Figure 6 (a)). The trend line of PWT in 2.5 mg/kg B14-treated BCP group demonstrated slight differences in contrast with vehicle-treated BCP rats ($F_{5,54} = 295.2$, $p > 0.05$, $*p < 0.05$ vs. control; $n = 10$, two-way repeated measures ANOVA, Figure 6(a)).

In long-term treatment, PWT of the operation side on days 0, 3, 6, 9, 12, 15, and 18 after surgery was recorded after reaching the peak value. The speed of declination of mechanical allodynia was slowed down in BCP (5 mg/kg and 10 mg/kg) group during the treatment (from day 6 to day 12) ($F_{5,54} = 185.1$, $***p < 0.001$ vs. control; $n = 10$, two-way repeated measures ANOVA, Figure 6 (b)). Similar trend was not observed in the BCP (2.5 mg/kg) group after treatment ($F_{5,54} = 185.1$, $p > 0.05$ vs. control; $n = 10$, two-way repeated measures ANOVA, Figure 6(b)).

I.p. injection of B14 inhibits the activation of JAK2/STAT3 in nerve cells and downregulates the expression of IL-1 β

The ratio of p-JAK2/JAK2 showed progressive declination with an increasing doses of B14 ($F_{5,18} = 25.98$, $\#p < 0.05$, $\#\#p < 0.01$ vs. control; $n = 4$, one-way ANOVA, Figure 7(e) and (f)). An analogous tendency was present in the rate of p-STAT3/STAT3 in spinal tissues ($F_{5,18} = 38.17$, $\#\#\#p < 0.001$ vs. control; $n = 4$, one-way ANOVA, Figure 8(e) and (f)). The protein levels of IL-1 β was downregulated with gradual increase of B14 ($F_{5,18} = 19.44$, $\#p < 0.05$, $\#\#p < 0.01$ vs. control; $n = 4$, one-way ANOVA, Figure 9(e) and (f)). When the B14 concentration was 2.5 mg/kg, the secretion of IL-1 β was remain unchanged ($F_{5,18} = 19.44$, $p > 0.05$ vs. control; $n = 4$, one-way ANOVA, Figure 9(e) and (f)). At a concentration of 2.5 mg/kg, B14 demonstrated no impact on the

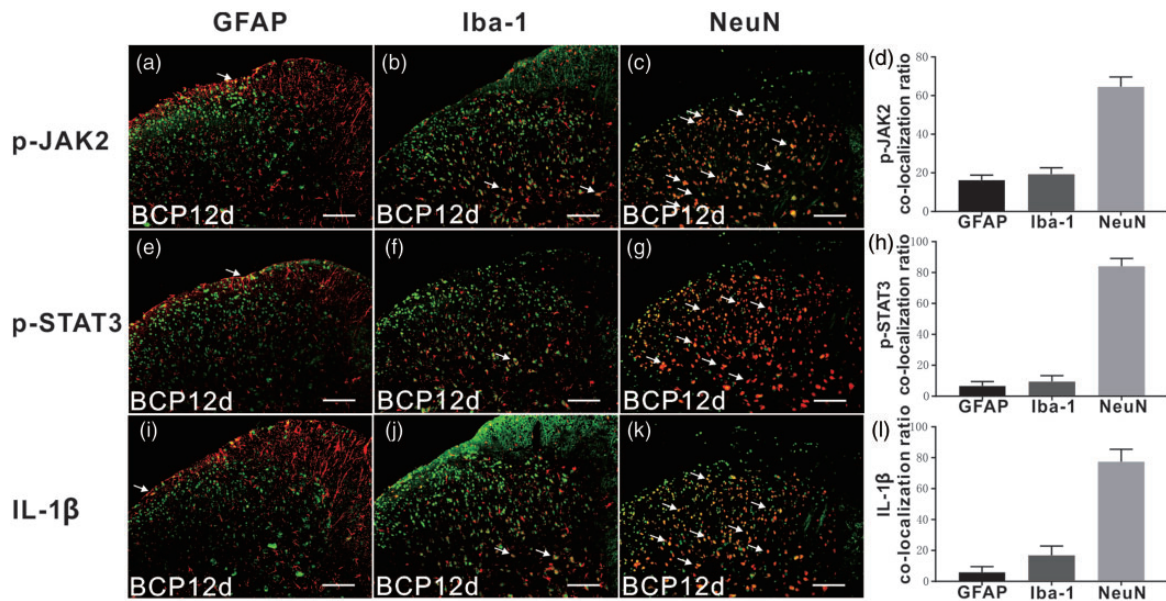


Figure 5. P-JAK2, p-STAT3, and IL-1 β cellular colocalization in spinal cord dorsal horn at BCP 12 days. Double immunostaining showing p-JAK2 was colocalized with astrocyte (a), microglial cell (b) and neuron (c), most colocalized with neuron almost 64.5% \pm 4.8%; 16.3% \pm 2.4% p-JAK2 colocalized with astrocyte, with microglial cell around 19.3% \pm 3.6% (d). Double immunostaining also showing p-STAT3 was colocalized with astrocyte (d), microglial cell (e), and neuron (f), 84.0% \pm 4.8% colocalized with neuron, 6.6% \pm 2.6% with astrocyte, 9.4% \pm 3.6% with microglial cell (h). The result of IL-1 β cellular colocalization in spinal cord dorsal horn revealed IL-1 β colocalized mostly with neuron (k) 77.4% \pm 7.6% (l), rather astrocyte (i) 5.9% \pm 3.4% (l) or microglial cell (j) 16.8% \pm 5.7% (l), $n = 10$ per group. Scale bar: 100 μ m. BCP: bone cancer pain; IL: interleukin; JAK2: janus-activated kinase 2; STAT3: signal transducer and activator of transcription 3; GFAP: glial fibrillary acidic protein.

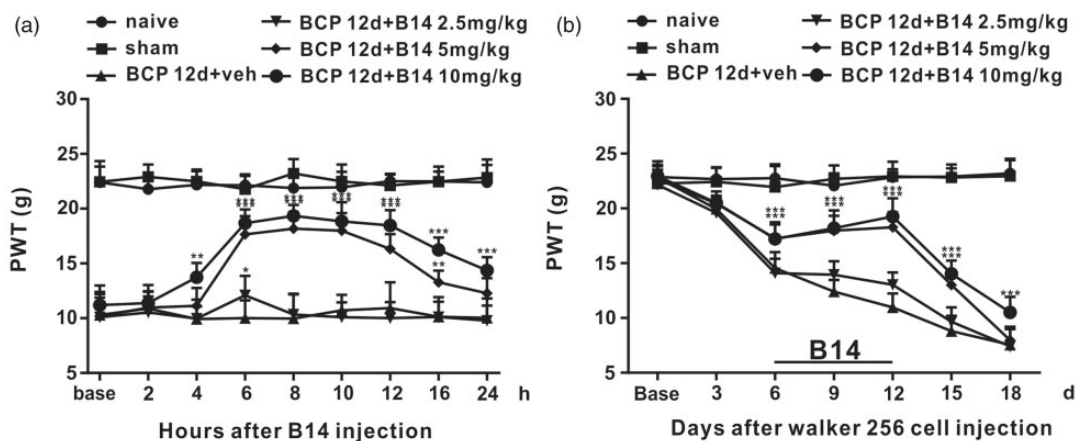


Figure 6. Single intraperitoneal administration and multiple intraperitoneal administration of B14 influence on mechanical allodynia in BCP molding. (a) At BCP 12 days, single dose of various concentrations of B14 were given to corresponding group. Injection of 5 mg/kg and 10 mg/kg B14 significantly alleviated pain caused by BCP molding, lasting roughly 6 h, $n = 10$ per group, $***p < 0.001$, $**p < 0.001$ versus BCP 12 days + veh group. (b) Multiple dose of various concentrations of B14 were given from BCP 6 days to BCP 12 days. During administration, mechanical withdrawal threshold of BCP 12 days + B14 5 mg/kg and BCP 12 days + B14 10 mg/kg groups were gradually raised, $n = 10$ per group, $***p < 0.001$, $**p < 0.001$ versus BCP 12 days + veh group. BCP: bone cancer pain; PWT: paw withdrawal threshold.

expression of p-JAK2 and p-STAT3 ($F_{5,18} = 25.98$, $p > 0.05$ vs. control; $n = 4$, $F_{5,18} = 38.17$, $p > 0.05$ vs. control; one-way ANOVA, Figures 7(e) and (f) and 8(e) and (f).

The pharmacological effects of B14 on p-JAK2, p-STAT3, and IL-1 β in cornu dorsale medullae spinalis were redemonstrated via immunofluorescence. The intumescentia lumbalis (L3–L5) sample was acquired from

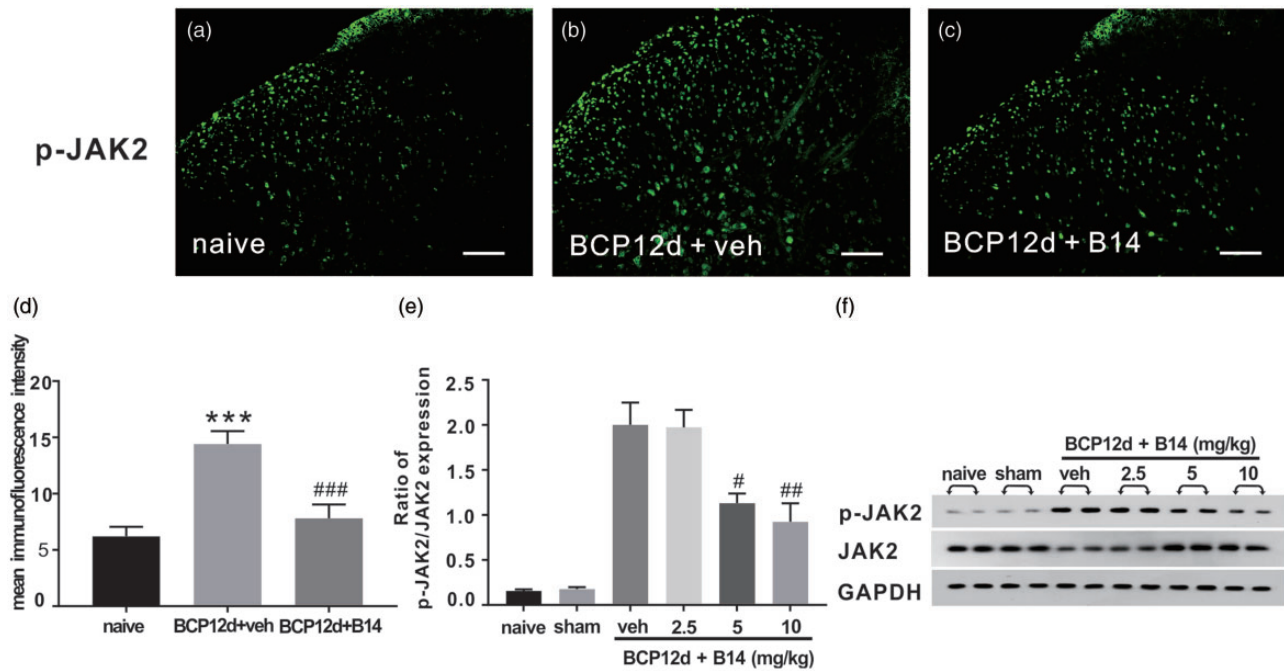


Figure 7. B14 impact the escalating trend of p-JAK2 in BCP molding. (a to d) Immunofluorescence results shown the expression of p-JAK was increased in control group and multiple intraperitoneal administration of B14 (10 mg/kg) remarkably decreased the expression of p-JAK, $n = 10$ per group, $***p < 0.001$, $###p < 0.001$ versus sham group. (e and f) Western blot analysis shown multiple intraperitoneal administration of B14 5 mg/kg and 10 mg/kg markedly cut down the protein level of p-JAK2 in spinal cord, $n = 4$ per group, $#p < 0.05$, $##p < 0.01$ versus sham group. But in the concentration at 2.5 mg/kg, the effect was limited, $n = 4$ per group, $p > 0.05$ versus sham group. Scale bar: 100 μm . BCP: bone cancer pain; JAK2: janus-activated kinase 2; GAPDH: glyceraldehyde 3-phosphate dehydrogenase.

naive, sham, and 10 mg/kg B14-treated BCP groups on day 12 after operation. Under fluorescence microscope, the locations of these factors were detected. The mean immunofluorescence intensity of p-JAK2 and p-STAT3 in sham group was much stronger than those in 10 mg/kg B14-treated BCP group ($F_{2,27} = 35.04$, $###p < 0.001$ vs. control; $F_{2,27} = 56.49$, $###p < 0.001$ vs. control; $n = 10$, one-way ANOVA, Figures 7(a) to (d) and 8(a) to (d)). From IL-1 β immunofluorescence images, a noteworthy gap between control and 10 mg/kg B14-treated BCP groups was observed ($F_{2,27} = 85.6$, $###p < 0.001$ vs. control; $n = 10$, one-way ANOVA, Figure 9(a) to (d)), which was in parallel to the analysis of Western blotting (Figure 9(e) and (f)).

Discussion

In this study, we demonstrated that (a) the ratio of p-JAK2/JAK2 and p-STAT3/STAT3 and the level of IL-1 β were increased after transplantation in Walker 256 cells; (b) p-JAK2, p-STAT3, and IL-1 β were over-expressed in the neurons of spinal cord dorsal horn as shown by immunofluorescence; (c) acute or chronic i.p. injection of B14 relieved BCP; and (d) i.p. injection of

B14 suppressed the activation of JAK2/STAT3 signaling pathway and downregulated the expression of IL-1 β .

Our previous studies have already proven that bone cancer-induced hyperpathia was triggered by activating protein kinase C-directed phosphorylation of HMGB1. HMGB1 phosphorylation caused translocation of itself from the nucleus in the spinal dorsal horn, activating inflammatory cascade falls.³⁸ Besides, we have also demonstrated that NF- κB pathway influenced the cancer-induced bone pain by regulating the levels of MCP-1/CCR2-dependent inflammatory factors.³⁷

JAK2/STAT3 signaling path is a well-known pathway in inflammation.^{45,46} In this study, we showed that the ratios of p-JAK2/JAK2 and p-STAT3/STAT3 were increased in the spinal cord of BCP rats on day 6. According to a recent study, the upregulation of p-JAK2 and p-STAT3 occurred on day 14, which was similar to our results.⁴⁷ The variation tendency of p-JAK2/JAK2 ratio and p-STAT3/STAT3 ratio was similar to that of our previous research, which was increased from days 12 to 18.^{48,49} IL-1 β is a downstream inflammatory factor of JAK3/STAT3 signaling pathway.²⁹ Former research papers reported that IL-1 β has the ability to act as a neurotoxic mediator,³⁰ while few others demonstrated that IL-1 β mediated neuronal apoptosis via p-38

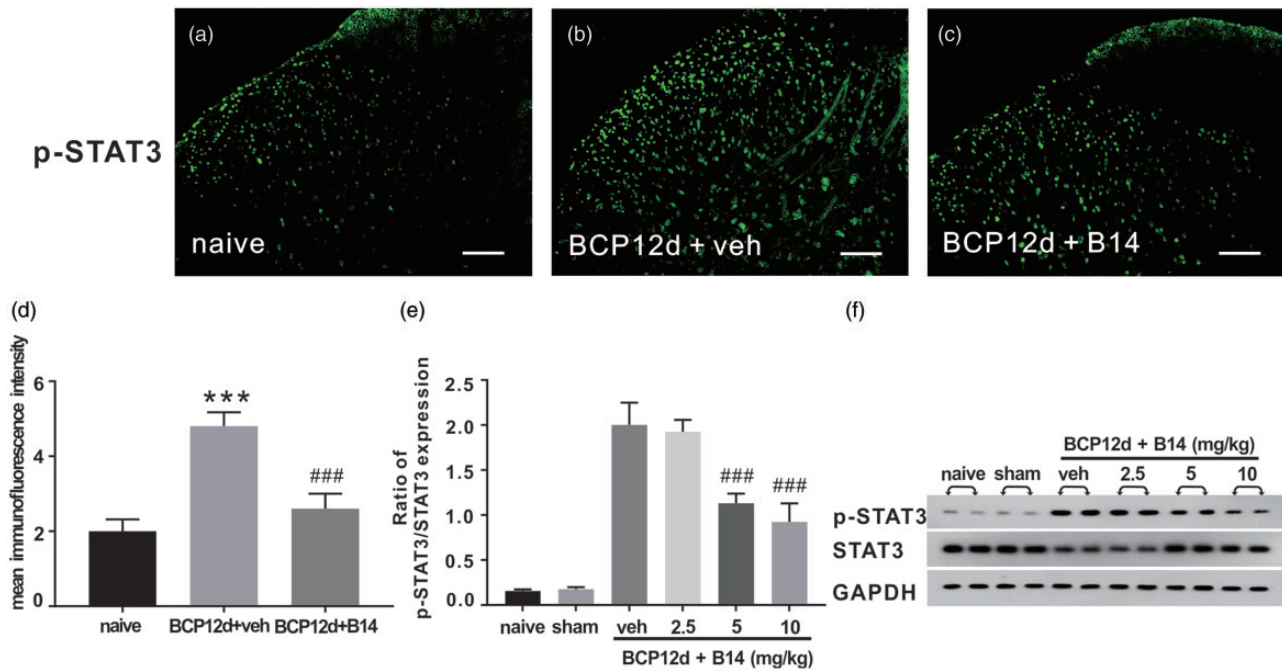


Figure 8. B14 impact the escalating trend of p-STAT3 in BCP molding. (a to d) Immunofluorescence results shown the expression of p-STAT3 was increased in control group and multiple intraperitoneal administration of B14 (10 mg/kg) remarkably decreased the expression of p-STAT3, $n = 10$ per group, $***p < 0.001$, $####p < 0.001$ versus sham group. (e and f) Western blot analysis shown multiple intraperitoneal administration of B14 5 mg/kg and 10 mg/kg markedly cut down the protein level of p-STAT3 in spinal cord, $n = 4$ per group, $####p < 0.001$, $####p < 0.001$ versus sham group. On the contrary, at 2.5 mg/kg, B14 made no difference on the result, $n = 4$ per group, $p > 0.05$ versus sham group. Scale bar: 100 μm . BCP: bone cancer pain; STAT3: signal transducer and activator of transcription 3; GAPDH: glyceraldehyde 3-phosphate dehydrogenase.

mitogen-activated protein kinase activity after spinal cord injury.³² Here, IL-1 β expression showed an increase in the spinal tissues of BCP rats, which was consistent with other research studies.^{50,51}

Many previous research studies indicated that upregulated p-JAK2 and p-STAT3 were probed in astrocytes and tremendously participated in the activation of astrocytes in the spinal horn of neuropathic pain model.^{44,52} A rapidly growing body of evidence showed that microglial cells are critical components for hyperpathia and coexistence of STAT3 with microglia.^{53,54} Our current immunofluorescence results showed that p-JAK2 and p-STAT3 were activated by BCP colocalized with astrocytes, microglial cells, and neurons in spinal dorsal horn. Vast majority of these proteins were located on the neurons, which may in turn cause hyperexcitability of neurons. Apparently, the double-labeled immunofluorescence results were not in line with the prevailing view but were still consistent with some other former studies.^{55,56} Similarly, the enhanced IL-1 β expression was detected on the neurons of BCP rats, aggravating inflammation of spinal dorsal horn. We must admit that a large number of studies showed that astroglia or microglia secreted IL-1 β activated neurons through IL-1R during inflammation or neuropathic pain. However,

there are also studies that demonstrated growth factor deprivation, oxidative stress, which other studies demonstrated intraneuronal Nlrp1 inflammasome activation to caspase-1-generated IL-1 β -mediated neuroinflammation.⁵⁷ Other research studies showed that neurons have secreted IL-1 β -activated microglia and astroglial,⁵⁸ which was consistent with our study result.

Curcumin is an effective extract of turmeric that is widely used and studied in many areas. Unfortunately, due to its natural features such as low bioavailability and solubility, poor chemical stability, high metabolic rate, and so on, its extensive use in clinics was limited. For this reason, in our experiment, we used B14, which is a curcumin analogue and has better performance.⁵⁹ Similarly, during the exploration of psoriasis treatment by cobinding of hyaluronic acid with propylene glycol-based ethosomes, a new type of carrier for curcumin has been invented.⁶⁰ Nanocurcumin is manufactured for the treatment of cerebral ischemia–reperfusion injury.⁶¹ In the clinical trial of Alzheimer's disease, curcumin 4 g/day was given to patients for 24 weeks as a course of treatment.⁶² In animal models of neuropathic pain induced by diabetes or mechanical injury, 45 mg/kg and 60 mg/kg of curcumin twice a day were given for four weeks.⁶³ Other recent studies confirmed that doses of 60 mg/kg

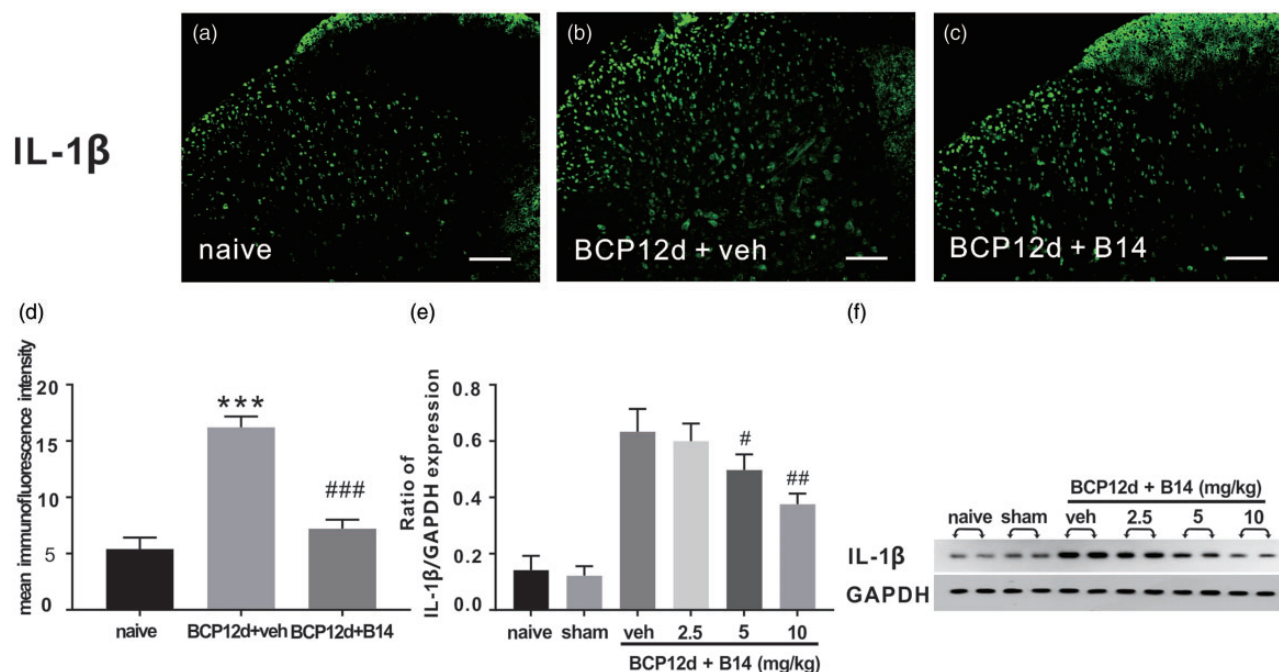


Figure 9. B14 impact the escalating trend of IL-1 β in BCP molding. (a to d) Immunofluorescence results shown the expression of IL-1 β was increased in control group and multiple intraperitoneal administration of B14 (10 mg/kg) remarkably decreased the expression of IL-1 β , $n = 10$ per group, *** $p < 0.001$, ### $p < 0.001$ versus sham group. (e and f) Western blot analysis shown multiple intraperitoneal administration of B14 5 mg/kg and 10 mg/kg markedly cut down the protein level of IL-1 β in spinal cord, $n = 4$ per group, # $p < 0.05$, ## $p < 0.01$ versus sham group. When the concentration was 2.5 mg/kg, the secretion of IL-1 β was not affected, $n = 4$ per group, $p > 0.05$ versus sham group. Scale bar: 100 μm . BCP: bone cancer pain; GAPDH: glyceraldehyde 3-phosphate dehydrogenase; IL: interleukin.

and 120 mg/kg curcumin markedly alleviated SNI-induced mechanical allodynia, while the dose of 30 mg/kg showed no difference in pain.⁶⁴ In our experiment, three doses of B14 (2.5, 5, and 10 mg/kg) were given once a day continuously for one week, which significantly mitigated cancer-induced bone pain in rats (except 2.5 mg/kg). Meanwhile, the results of Western blotting and immunofluorescence demonstrated that i.p. injection of B14 remarkably downregulated the expressions of p-JAK2, p-STAT3, and IL-1 β .

In a study conducted on BCP mice, a new drug DR-1-55 suppressed the expression of p-STAT3, leading to a decrease in human IL-6 and IL1-1 β secreted by T47D clones by relieving cancer-induced bone pain.⁶⁵ In an experiment on spinal cord injury, curcumin treatment inhibited the activation of STAT3 and NF- κ B, while the levels of IL-1 β and nitric oxide were severely reduced.⁶⁶ In cerebral ischemic model, curcumin suppressed the activation of JAK2/STAT3, decreased HMGB1, and decreased the expression of inflammatory factors such as IL-1 β , tumor necrosis factor- α . Therefore, B14, which is an analogue of curcumin, inhibited the activation of JAK2/STAT3 signaling pathway, leading to the downregulation of the expression of IL-1 β in spinal neurons, eventually lightening the pain of bone cancer. Furthermore, other action sites and side effects of B14 required deeper and

thorough study. But one of the biggest regrets of this experiment is that we did not explore the specific interaction sites of B14, which is worthy investigation in future.

Conclusion

In this study, we proved that JAK2 and STAT3 phosphorylation was significantly increased during the development of BCP and is accompanied by gradual upregulation of IL-1 β . B14 treatment remarkably alleviated BCP by downregulating spinal IL-1 β via suppression of neuronal JAK2/STAT3 signaling pathway.

Acknowledgments

The authors thank Renshan Ge (Wenzhou Medical University, China) for proofreading the paper.

Authors' Contributions

XM designed and scheduled the study. XM performed the experiments. YGW and HSD participated in part of the BCP modeling and behavioral testing. HS guided the immunofluorescent staining and Western blot. LSX and MY supervised the experiments. XM and HDN wrote the article.

Data Accessibility Statement

All data generated or analyzed during this study are included in this published article.

Declaration of Conflicting Interests

The author(s) declared no potential conflicts of interest with research, authorship, and/or publication of this article.

Funding

The author(s) disclosed receipt of the following financial support for the research, authorship, and/or publication of this article: This study was supported, in part, by grants from the National Science Foundation for Young Scientists of China (81901124), the Natural Science Foundation of Zhejiang Province (LY17H090019 and LQ19H090007), the Science and Technology Project of Jiaxing City (2018AY32012), Medical Scientific Research Foundation of Zhejiang Province, China (2020358554 and 2020RC122), the Medical and Health General Research Program of Zhejiang Province (2019KY687), the Construction Project of Anesthesiology Discipline Special Disease Center in Zhejiang North Region (201524), the Key Medical Subjects Established by Zhejiang Province and Jiaxing City Jointly Pain Medicine (2019-ss-ttyx), and the Construction Project of Key Laboratory of Nerve and Pain Medicine in Jiaxing City. They also thank Professor Renshan Ge, the former head of the Endocrinology Lab of the CBR in Population Council (USA), for English language editing.

ORCID iD

Ming Yao  <https://orcid.org/0000-0002-4226-8473>

References

1. Frost CO, Hansen RR, Heegaard AM. Bone pain: current and future treatments. *Curr Opin Pharmacol* 2016; 28: 31–37.
2. Mantyh P. Bone cancer pain: causes, consequences, and therapeutic opportunities. *Pain* 2013; 154: S54–S62.
3. Kane CM, Hoskin P, Bennett MI. Cancer induced bone pain. *BMJ* 2015; 350: h315.
4. Zhang N, Yan F, Liang X, Wu M, Shen Y, Chen M, Xu Y, Zou G, Jiang P, Tang C, Zheng H, Dai Z. Localized delivery of curcumin into brain with polysorbate 80-modified cerasomes by ultrasound-targeted microbubble destruction for improved Parkinson's disease therapy. *Theranostics* 2018; 8: 2264–2277.
5. Kesharwani SS, Ahmad R, Bakkari MA, Rajput MKS, Dachineni R, Valiveti CK, Kapur S, Jayarama Bhat G, Singh AB, Tummala H. Site-directed non-covalent polymer-drug complexes for inflammatory bowel disease (IBD): formulation development, characterization and pharmacological evaluation. *J Control Release* 2018; 290: 165–179.
6. Jung E, Noh J, Kang C, Yoo D, Song C, Lee D. Ultrasound imaging and on-demand therapy of peripheral arterial diseases using H₂O₂-activated bubble generating anti-inflammatory polymer particles. *Biomaterials* 2018; 179: 175–185.
7. Jiang T-F, Zhang Y-J, Zhou H-Y, Wang H-M, Tian L-P, Liu J, Ding J-Q, Chen S-D. Curcumin ameliorates the neurodegenerative pathology in A53T α synuclein cell model of Parkinson's disease through the downregulation of mTOR p70S6K signaling and the recovery of macroautophagy. *J Neuroimmune Pharmacol* 2013; 8: 356–369.
8. Serafini MM, Catanzaro M, Rosini M, Racchi M, Lanni C. Curcumin in Alzheimer's disease: can we think to new strategies and perspectives for this molecule? *Pharmacol Res* 2017; 124: 146–155.
9. Wang YJ, Thomas P, Zhong JH, Bi FF, Kosaraju S, Pollard A, Fenech M, Zhou XF. Consumption of grape seed extract prevents amyloid-beta deposition and attenuates inflammation in brain of an Alzheimer's disease mouse. *Neurotox Res* 2009; 15: 3–14.
10. Fan Z, Li J, Liu J, Jiao H, Liu B. Anti-inflammation and joint lubrication dual effects of a novel hyaluronic acid/curcumin nanomicelle improve the efficacy of rheumatoid arthritis therapy. *ACS Appl Mater Interfaces* 2018; 10: 23595–23604.
11. Sharman MJ, Gyengesi E, Liang H, Chatterjee P, Karl T, Li QX, Wenk MR, Halliwell B, Martins RN, Munch G. Assessment of diets containing curcumin, epigallocatechin-3-gallate, docosahexaenoic acid and alpha-lipoic acid on amyloid load and inflammation in a male transgenic mouse model of Alzheimer's disease: are combinations more effective? *Neurobiol Dis* 2019; 124: 505–519.
12. den Haan J, Morrema THJ, Verbraak FD, de Boer JF, Scheltens P, Rozemuller AJ, Bergen AAB, Bouwman FH, Hoozemans JJ. Amyloid-beta and phosphorylated tau in post-mortem Alzheimer's disease retinas. *Acta Neuropathol Commun* 2018; 6: 147.
13. Mollazadeh H, Cicero AFG, Blesso CN, Pirro M, Majeed M, Sahebkar A. Immune modulation by curcumin: the role of interleukin-10. *Crit Rev Food Sci Nutr* 2019; 59: 89–101.
14. Cunha Neto F, Marton LT, de Marqui SV, Lima TA, Barbalho SM. Curcuminoids from *Curcuma Longa*: new adjuvants for the treatment of Crohn's disease and ulcerative colitis? *Crit Rev Food Sci Nutr* 2019; 59: 2136–2143.
15. Liang G, Yang S, Jiang L, Zhao Y, Shao L, Xiao J, Ye F, Li Y, Li X. Synthesis and anti-bacterial properties of mono-carbonyl analogues of curcumin. *Chem Pharm Bull (Tokyo)* 2008; 56: 162–167.
16. Liang G, Zhou H, Wang Y, Gurley EC, Feng B, Chen L, Xiao J, Yang S, Li X. Inhibition of LPS-induced production of inflammatory factors in the macrophages by mono-carbonyl analogues of curcumin. *J Cell Mol Med* 2009; 13: 3370–3379.
17. Imada K, Leonard WJ. The Jak-STAT pathway. *Mol Immunol* 2000; 37: 1–11.
18. Li YY, Li H, Liu ZL, Li Q, Qiu HW, Zeng LJ, Yang W, Zhang XZ, Li ZY. Activation of STAT3-mediated CXCL12 up-regulation in the dorsal root ganglion contributes to oxaliplatin-induced chronic pain. *Mol Pain* 2017; 13: 174480691774742.

19. Dell'Albani P, Santangelo R, Torrisi L, Nicoletti VG, Giuffrida Stella AM. Role of the JAK/STAT signal transduction pathway in the regulation of gene expression in CNS. *Neurochem Res* 2003; 28: 53–64.
20. Lim G, Wang S, Zhang Y, Tian Y, Mao J. Spinal leptin contributes to the pathogenesis of neuropathic pain in rodents. *J Clin Invest* 2009; 119: 295–304.
21. Tian Y, Wang S, Ma Y, Lim G, Kim H, Mao J. Leptin enhances NMDA-induced spinal excitation in rats: a functional link between adipocytokine and neuropathic pain. *Pain* 2011; 152: 1263–1271.
22. Li D, Yan Y, Yu L, Duan Y. Procaine attenuates pain behaviors of neuropathic pain model rats possibly via inhibiting JAK2/STAT3. *Biomol Ther (Seoul)* 2016; 24: 489–494.
23. Liu S, Mi WL, Li Q, Zhang MT, Han P, Hu S, Mao-Ying QL, Wang YQ. Spinal IL-33/ST2 signaling contributes to neuropathic pain via neuronal CaMKII-CREB and astroglial JAK2-STAT3 cascades in mice. *Anesthesiology* 2015; 123: 1154–1169.
24. Lee SY, Lee SH, Na HS, Kwon JY, Kim GY, Jung K, Cho KH, Kim SA, Go EJ, Park MJ, Baek JA, Choi SY, Jhun J, Park SH, Kim SJ, Cho ML. The therapeutic effect of STAT3 signaling-suppressed MSC on pain and articular cartilage damage in a rat model of monosodium iodoacetate-induced osteoarthritis. *Front Immunol* 2018; 9: 2881.
25. Liu H, Wei J, Liu M, Wu S, Ma C, Liu C, Huang K, Zhang X, Guo R, Zhang K, Xin W. Epigenetic upregulation of CXCL12 expression contributes to the acquisition and maintenance of morphine-induced conditioned place preference. *Exp Neurol* 2018; 306: 55–63.
26. Erlandsson MC, Toyra Silfversward S, Nadali M, Turkmila M, Svensson MND, Jonsson IM, Andersson KME, Bokarewa MI. IGF-1R signalling contributes to IL-6 production and T cell dependent inflammation in rheumatoid arthritis. *Biochim Biophys Acta Mol Basis Dis* 2017; 1863: 2158–2170.
27. Doyle TM, Chen Z, Durante M, Salvemini D. Activation of sphingosine-1-phosphate receptor 1 in the spinal cord produces mechano-hypersensitivity through the activation of inflammasome and IL-1beta pathway. *J Pain* 2019; 19: 26.
28. Liu S, Li Q, Zhang MT, Mao-Ying QL, Hu LY, Wu GC, Mi WL, Wang YQ. Curcumin ameliorates neuropathic pain by down-regulating spinal IL-1beta via suppressing astroglial NALP1 inflammasome and JAK2-STAT3 signalling. *Sci Rep* 2016; 6: 28956.
29. Chen Z, Liu Y, Sun B, Li H, Dong J, Zhang L, Wang L, Wang P, Zhao Y, Chen C. Polyhydroxylated metallofullerenols stimulate IL-1beta secretion of macrophage through TLRs/MyD88/NF-kappaB pathway and NLRP(3) inflammasome activation. *Small* 2014; 10: 2362–2372.
30. Clausen F, Hanell A, Israelsson C, Hedin J, Ebendal T, Mir AK, Gram H, Marklund N. Neutralization of interleukin-1beta reduces cerebral edema and tissue loss and improves late cognitive outcome following traumatic brain injury in mice. *Eur J Neurosci* 2011; 34: 110–123.
31. Carvey PM, Chen EY, Lipton JW, Tong CW, Chang QA, Ling ZD. Intra-parenchymal injection of tumor necrosis factor-alpha and interleukin 1-beta produces dopamine neuron loss in the rat. *J Neural Transm* 2005; 112: 601–612.
32. Wang XJ, Kong KM, Qi WL, Ye WL, Song PS. Interleukin-1 beta induction of neuron apoptosis depends on p38 mitogen-activated protein kinase activity after spinal cord injury. *Acta Pharmacol Sin* 2005; 26: 934–942.
33. Bavarsad K, Barreto GE, Hadjzadeh MA, Sahebkar A. Protective effects of curcumin against ischemia-reperfusion injury in the nervous system. *Mol Neurobiol* 2019; 56: 1391–1404.
34. Zhou YQ, Liu Z, Liu HQ, Liu DQ, Chen SP, Ye DW, Tian YK. Targeting glia for bone cancer pain. *Expert Opin Ther Targets* 2016; 20: 1365–1374.
35. Starobova H, Vetter I. Pathophysiology of chemotherapy-induced peripheral neuropathy. *Front Mol Neurosci* 2017; 10: 174.
36. Huo W, Liu Y, Lei Y, Zhang Y, Huang Y, Mao Y, Wang C, Sun Y, Zhang W, Ma Z, Gu X. Imbalanced spinal infiltration of Th17/Treg cells contributes to bone cancer pain via promoting microglial activation. *Brain Behav Immun* 2019; 79: 139–151.
37. Wang Y, Ni H, Li H, Deng H, Xu LS, Xu S, Zhen Y, Shen H, Pan H, Yao M. Nuclear factor kappa B regulated monocyte chemoattractant protein-1/chemokine CC motif receptor-2 expressing in spinal cord contributes to the maintenance of cancer-induced bone pain in rats. *Mol Pain* 2018; 14: 174480691878868.
38. An K, Rong H, Ni H, Zhu C, Xu L, Liu Q, Chen Y, Zheng Y, Huang B, Yao M. Spinal PKC activation-induced neuronal HMGB1 translocation contributes to hyperalgesia in a bone cancer pain model in rats. *Exp Neurol* 2018; 303: 80–94.
39. Zimmermann M. Ethical guidelines for investigations of experimental pain in conscious animals. *Pain* 1983; 16: 109–110.
40. Yao M, Chang XY, Chu YX, Yang JP, Wang LN, Cao HQ, Liu MJ, Xu QN. Antiallodynic effects of propentofylline elicited by interrupting spinal glial function in a rat model of bone cancer pain. *J Neurosci Res* 2011; 89: 1877–1886.
41. Mao-Ying QL, Zhao J, Dong ZQ, Wang J, Yu J, Yan MF, Zhang YQ, Wu GC, Wang YQ. A rat model of bone cancer pain induced by intra-tibia inoculation of Walker 256 mammary gland carcinoma cells. *Biochem Biophys Res Commun* 2006; 345: 1292–1298.
42. Kou ZZ, Wan FP, Bai Y, Li CY, Hu JC, Zhang GT, Zhang T, Chen T, Wang YY, Li H, Li YQ. Decreased endomorphin-2 and mu-opioid receptor in the spinal cord are associated with painful diabetic neuropathy. *Front Mol Neurosci* 2016; 9: 80.
43. Fox A, Medhurst S, Courade J-P, Glatt M, Dawson J, Urban L, Bevan S, Gonzalez I. Anti-hyperalgesic activity of the cox-2 inhibitor lumiracoxib in a model of bone cancer pain in the rat. *Pain* 2004; 107: 33–40.
44. Tsuda M, Kohro Y, Yano T, Tsujikawa T, Kitano J, Tozaki-Saitoh H, Koyanagi S, Ohdo S, Ji RR, Salter MW, Inoue K. JAK-STAT3 pathway regulates spinal

- astrocyte proliferation and neuropathic pain maintenance in rats. *Brain* 2011; 134: 1127–1139.
45. Adan N, Guzman-Morales J, Ledesma-Colunga MG, Perales-Canales SI, Quintanar-Stephano A, Lopez-Barrera F, Mendez I, Moreno-Carranza B, Triebel J, Binart N, Martinez de la Escalera G, Thebault S, Clapp C. Prolactin promotes cartilage survival and attenuates inflammation in inflammatory arthritis. *J Clin Invest* 2013; 123: 3902–3913.
 46. Zhou GY, Yi YX, Jin LX, Lin W, Fang PP, Lin XZ, Zheng Y, Pan CW. The protective effect of juglanin on fructose-induced hepatitis by inhibiting inflammation and apoptosis through TLR4 and JAK2/STAT3 signaling pathways in fructose-fed rats. *Biomed Pharmacother* 2016; 81: 318–328.
 47. Chen SP, Sun J, Zhou YQ, Cao F, Braun C, Luo F, Ye DW, Tian YK. Sinomenine attenuates cancer-induced bone pain via suppressing microglial JAK2/STAT3 and neuronal CAMKII/CREB cascades in rat models. *Mol Pain* 2018; 14: 174480691879323.
 48. Sriram K, Benkovic SA, Hebert MA, Miller DB, O'Callaghan JP. Induction of gp130-related cytokines and activation of JAK2/STAT3 pathway in astrocytes precedes up-regulation of glial fibrillary acidic protein in the 1-methyl-4-phenyl-1,2,3,6-tetrahydropyridine model of neurodegeneration: key signaling pathway for astrogliosis in vivo? *J Biol Chem* 2004; 279: 19936–19947.
 49. Guo C-H, Bai L, Wu H-H, Yang J, Cai G-H, Zeng S-X, Wang X, Wu S-X, Ma W. Midazolam and ropivacaine act synergistically to inhibit bone cancer pain with different mechanisms in rats. *Oncol Rep* 2017; 37: 249–258.
 50. Liu M, Yao M, Wang H, Xu L, Zheng Y, Huang B, Ni H, Xu S, Zhou X, Lian Q. P2Y12 receptor-mediated activation of spinal microglia and p38MAPK pathway contribute to cancer-induced bone pain. *J Pain Res* 10: 417–426.
 51. Liu S, Yang J, Wang L, Jiang M, Qiu Q, Ma Z, Liu L, Li C, Ren C, Zhou J, Li W. Tibia tumor-induced cancer pain involves spinal p38 mitogen-activated protein kinase activation via TLR4-dependent mechanisms. *Brain Res* 2010; 1346: 213–223.
 52. Herrmann JE, Imura T, Song B, Qi J, Ao Y, Nguyen TK, Korsak RA, Takeda K, Akira S, Sofroniew MV. STAT3 is a critical regulator of astrogliosis and scar formation after spinal cord injury. *J Neurosci* 2008; 28: 7231–7243.
 53. Dominguez E, Rivat C, Pommier B, Mauborgne A, Pohl M. JAK/STAT3 pathway is activated in spinal cord microglia after peripheral nerve injury and contributes to neuropathic pain development in rat. *J Neurochem* 2008; 107: 50–60.
 54. Li CD, Zhao JY, Chen JL, Lu JH, Zhang MB, Huang Q, Cao YN, Jia GL, Tao YX, Li J, Cao H. Mechanism of the JAK2/STAT3-CAV-1-NR2B signaling pathway in painful diabetic neuropathy. *Endocrine* 2019; 64: 55–66.
 55. Chen K, Fan J, Luo ZF, Yang Y, Xin WJ, Liu CC. Reduction of SIRT1 epigenetically upregulates NALP1 expression and contributes to neuropathic pain induced by chemotherapeutic drug bortezomib. *J Neuroinflammation* 2018; 15: 292.
 56. Ding HH, Zhang SB, Lv YY, Ma C, Liu M, Zhang KB, Ruan XC, Wei JY, Xin WJ, Wu SL. TNF-alpha/STAT3 pathway epigenetically upregulates Nav1.6 expression in DRG and contributes to neuropathic pain induced by L5-VRT. *J Neuroinflammation* 2019; 16: 29.
 57. Kaushal V, Dye R, Pakavathkumar P, Foveau B, Flores J, Hyman B, Ghetti B, Koller BH, LeBlanc AC. Neuronal NLRP1 inflammasome activation of Caspase-1 coordinately regulates inflammatory interleukin-1-beta production and axonal degeneration-associated Caspase-6 activation. *Cell Death Differ* 2015; 22: 1676–1686.
 58. Shaftel SS, Griffin WS, O'Banion MK. The role of interleukin-1 in neuroinflammation and Alzheimer disease: an evolving perspective. *J Neuroinflammation* 2008; 5: 7.
 59. Liang G, Li X, Chen L, Yang S, Wu X, Studer E, Gurley E, Hylemon PB, Ye F, Li Y, Zhou H. Synthesis and anti-inflammatory activities of mono-carbonyl analogues of curcumin. *Bioorg Med Chem Lett* 2008; 18: 1525–1529.
 60. Zhang Y, Xia Q, Li Y, He Z, Li Z, Guo T, Wu Z, Feng N. CD44 assists the topical anti-psoriatic efficacy of curcumin-loaded hyaluronan-modified ethosomes: a new strategy for clustering drug in inflammatory skin. *Theranostics* 2019; 9: 48–64.
 61. Wang Y, Luo J, Li SY. Nano-curcumin simultaneously protects the blood-brain barrier and reduces M1 microglial activation during cerebral ischemia-reperfusion injury. *ACS Appl Mater Interfaces* 2019; 11: 3763–3770.
 62. Ringman JM, Frautschy SA, Teng E, Begum AN, Bardens J, Beigi M, Gylys KH, Badmaev V, Heath DD, Apostolova LG, Porter V, Vanek Z, Marshall GA, Hellemann G, Sugar C, Masterman DL, Montine TJ, Cummings JL, Cole GM. Oral curcumin for Alzheimer's disease: tolerability and efficacy in a 24-week randomized, double blind, placebo-controlled study. *Alzheimers Res Ther* 2012; 4: 43.
 63. Sharma S, Kulkarni SK, Agrewala JN, Chopra K. Curcumin attenuates thermal hyperalgesia in a diabetic mouse model of neuropathic pain. *Eur J Pharmacol* 2006; 536: 256–261.
 64. Das L, Vinayak M. Curcumin attenuates carcinogenesis by down regulating proinflammatory cytokine interleukin-1 (IL-1alpha and IL-1beta) via modulation of AP-1 and NF-IL6 in lymphoma bearing mice. *Int Immunopharmacol* 2014; 20: 141–147.
 65. Linher-Melville K, Sharma M, Nakhla P, Kum E, Ungard R, Park J, Rosa D, Gunning P, Singh G. Inhibiting STAT3 in a murine model of human breast cancer-induced bone pain delays the onset of nociception. *Mol Pain* 2019; 15:1744806918823477.
 66. Wang YF, Zu JN, Li J, Chen C, Xi CY, Yan JL. Curcumin promotes the spinal cord repair via inhibition of glial scar formation and inflammation. *Neurosci Lett* 2014; 560: 51–56.